Available online at www.sciencedirect.com
ScienceDirect
Chemical Physics Letters 433 (2007) 379–384
CHEMICAL PHYSICS LETTERS
www.elsevier.com/locate/cplett

Multiplex method for the measurement of nonlinear susceptibility spectrum applied to third-harmonic generation in a polydiacetylene

Takayoshi Kobayashi [a,b,c,d,*], Akihiro Mito [e], Satoshi Kobayashi [a], Takashi Taneichi [a,b], Atsuhiro Furuta [a]

[a] Department of Physics, The University of Tokyo, Hongo 7-3-1, Bunkyo-ku, Tokyo 113-0033, Japan
[b] Department of Applied Physics and Chemistry and Institute of Laser Science, The University of Telecommunications, Choufu-gaoka 1-5-1, Chofu, Tokyo 182-8585, Japan
[c] Institute of Laser Engineering, Osaka University, Yamadakami 2-6, Suita, 565-0871 Osaka, Japan
[d] Department of Electrophysics, National Chiao Tung University, 1001 Ta Hsueh Rd., Hsinchu 300, Taiwan
[e] National Institute of Advanced Industrial Science and Technology (AIST), Tsukuba Central 3, Tsukuba, Ibaraki 305-8563, Japan

Received 23 May 2006; in final form 6 November 2006
Available online 15 November 2006

Abstract

Broadband near-infrared pulse generated from NOPA (non-collinear optical parametric amplifier) was used for measurement of the spectrum of susceptibility of the third harmonic generation (THG). Corrections for the effects of absorption and refractive index, contribution of non-degenerate third-order nonlinearity, and THG by air, were properly addressed.

This multiplex method was applied to a polydiacetylene, poly[5,7-dodecadiyn-1,12-diol-bis(*n*-butoxylcarbonyl-methyl-urethane)] (4BCMU) in red phase resulting in a good agreement with theoretical prediction.

1. Introduction

Exact knowledge of the hyperpolarizabilities of organic molecules and polymers [1,2] is important for testing of molecular calculation, bond additivity of nonlinearity, nonlinear spectroscopy, and molecular interaction. Third-order nonlinear optical processes can be used for systems with any symmetry, in contrast to the lowest order nonlinear processes of the second-order, which are absent in systems with inversion symmetry [3–6].

Among the many third-order processes, third-harmonic (TH) generation (THG) is a purely electronic and coherent process, and no ambiguity in the mechanism in high contrast to other processes such as degenerate four-wave mixing and optical Kerr effect, in which other incoherent and coherent (like vibrational coherence) nonlinearities can contribute. Therefore, THG measurement is one of the simplest possible methods for the determination of $\chi^{(3)}$ allowing one to probe only electronic processes in a system. Hence THG $\chi^{(3)}$ spectrum is the most suitable for studying the mechanism of coherent electronic nonlinearity in a system.

Continuous spectrum of the susceptibility is desired to obtain information on the nonlinear susceptibility in the full spectral range of interest and requirement. For a conventional monochromatic laser, the wavelength of the laser must be tuned in a broad spectral range with a small step of wavelength. It takes very long time to get full data of the spectral response from which $\chi^{(3)}$ spectrum is calculated. In this case the results are expected to easily suffer from

* Corresponding author. Address: Department of Applied Physics and Chemistry and Institute of Laser Science, The University of Telecommunications, Choufu-gaoka 1-5-1, Chofu, Tokyo 182-8585, Japan. Fax: +81 42 443 5825.
E-mail address: kobayashi@ils.uec.ac.jp (T. Kobayashi).

0009-2614/$ - see front matter © 2006 Elsevier B.V. All rights reserved.
doi:10.1016/j.cplett.2006.11.025

errors induced by instability of the laser during the measurement time, differences in mode pattern and intensity of the fundamental radiation with different wavelengths from several lasers. It is therefore desired to study THG with a fundamental having a broad spectrum to obtain the $\chi^{(3)}$ spectrum of materials of interest.

In this paper, we propose a method for the measurement of $\chi^{(3)}$ utilizing a broadband pulse from a parametric amplifier pumped with a Ti–sapphire laser fundamental seeded with a femtosecond continuum.

2. Experimental

2.1. Measurement system

Fig. 1 shows a block diagram of the optical system for measurement of multiplex nonlinear susceptibility. The output from an Er-doped fiber mode-locked laser (Clark-MXR, SerF) was amplified with a thin sapphire regenerative amplifier (Clark-MXR, CPA-1000) and was used as a pump source of a parametric amplifier to generate a fundamental pulsed pump for THG. The repetition rate, center wavelength, pulse energy, and pulse duration of the output pulse were 1 kHz, 775 nm (1.6 eV), 0.5 mJ, and 160 fs, respectively. The polarization of the pulse was horizontal. Broadband near-infrared (IR) pulses were generated in the following way. The regenerative amplified pulse was split into two, the polarization of one of the pulses was converted to be vertical with a half-wave plate and then was focused with a lens of $f = 120$ cm into a 10 mm cell containing CCl_4 to generate white-light continuum.

The generated continuum was directed to a beta-barium borate (BBO, β-BaB_2O_4) crystal for use as a seed of an optical parametric amplifier (OPA). The OPA was pumped with a major fraction of the amplified pulse with a vertical polarization. The pump and white-light continuum were vertically and horizontally polarized and they were collinearly focused with a lens of 10 cm focal length to match the Type II phase-matching condition. This short focal length is feasible for a broad gain bandwidth of parametric amplification in a non-collinear configuration [7–9]. This is a novel type of non-collinear OPA (NOPA) aimed at generating extremely short pulses using broadband pulse developed by several groups including us [10–14].

The principle of generation of broadband near-IR pulse is as follows (Fig. 2). Since the short focal length lens is used for the amplifier, the signal continuum has a broad distribution of incident angle. Signals with different wavelength components incident with different angles to the nonlinear crystal generate an idler with different wavelengths. The idler spectrum was measured with a PtSi detector coupled to an IR polychromator. The idler had a spectrum extending from 0.46 eV (2.7 μm) to 0.78 eV (1.6 μm) corresponding to the wavelength of pump at 775 nm and that of femtosecond continuum generated in CCl_4extending from 0.9 to 1.6 μm.

The output pulse from the OPA composed of a signal and an idler was used as a pump for the THG. It was focused into a polymer film. The generated harmonic was guided to a polychromator ($f = 20$ cm, Ocean Optics) for a visible wavelength coupled to a CCD camera through an optical fiber. The spectral range of the combined system of the polychromator and detector extended from 320 to 1040 nm. The spectral resolution of the system was 3.0 nm with a slit width of 0.05 mm. The spectral sensitivities of the wavelength resolving detection systems in both visible and IR were corrected using a standard tungsten lamp (Ushio Electrics).

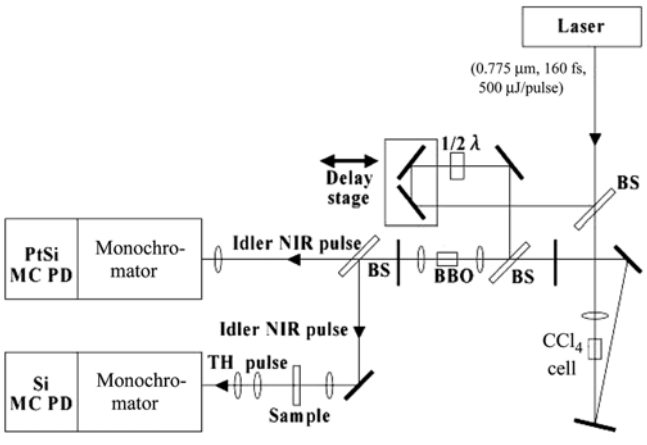

Fig. 1. Block diagram of apparatus for measurement of broadband multiplex TH spectrum. Laser: Ti–sapphire laser with a regenerative amplifier, BS: beam splitter, 1/2λ: half-wave plate, delay stage: variable optical stage, CCl_4 cell: a cell containing CCl_4 for femtosecond continuum generation, PtSi MC PD: PtSi multi-channel photodiode, and Si MC PD: Si multi-channel photodiode.

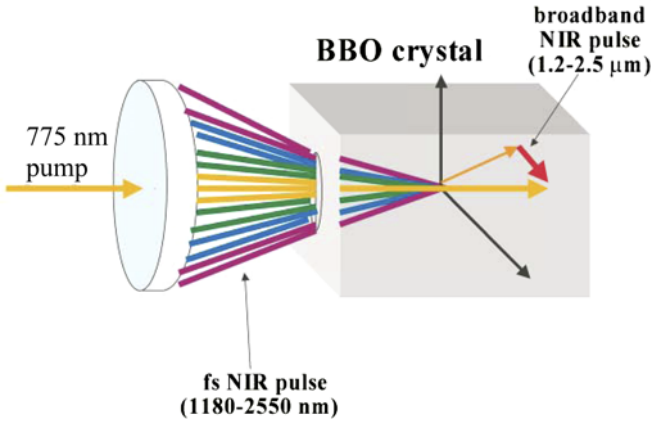

Fig. 2. Schematic figure of the broadband spectrum generation in near-IR by the OPA process. The generated white-light continuum is directed to a BBO crystal to be used as a seed of an OPA pumped with the amplified pulse with vertical polarization. The pump and white-light continuum are polarized vertically and horizontally, respectively, and the wave vectors at the beam center of both beams are collinearly focused by a lens with 10 cm focal length. This short focal length provides an angular dispersion in the femtosecond continuum resulting in a broad gain bandwidth of parametric amplification in the non-collinear configuration.

As a standard of the TH susceptibility, high-refractive index glass, FDS9, was used, which has high nonlinearity under non-resonant condition and availability of reliable absolute values of THG susceptibility. A very precise measurement with FDS9 and another high-refractive index glass, FD2, is reported [15]. The spectral dependence of the THG was reproduced by the present method of measurement. Therefore, these materials can be considered to be appropriate for the standards, and the present method has been verified to be reliable.

2.2. Sample

The sample, poly(4BCMU) [16], was provided by Drs. S. Shimada and H. Matsuda, National Institute of Advanced Industrial Science and Technology.

3. Method of the determination of the susceptibility

3.1. Correction of the effects of absorption and refractive index

THG takes place through the third-order nonlinear process. The nonlinear polarization is given as

$$P_{\mathrm{THG}} = \chi^{(3)}(-3\omega;\omega,\omega,\omega)E_\omega(r,t)E_\omega(r,t)E_\omega(r,t). \tag{1}$$

As the wavelength of incident pulse from the OPA extends from 0.9 to 2.7 μm, the TH wave is to be generated in the range of 0.3–0.9 μm. The polydiacetylene (PDA) sample used as a third-order nonlinear material has large absorption coefficients below 600 nm. Therefore, the absorption loss should be taken into account to obtain a correct third-order susceptibility. The position dependence of the intensity of TH, $I_{3\omega}$, is given by the following equation as a function of distance z from the incident plane of the nonlinear material and the linear absorption coefficient $\alpha_{3\omega}$ at the TH frequency:

$$\frac{\mathrm{d}I_{3\omega}}{\mathrm{d}z} = BC\sin 2Cz - \alpha_{3\omega}I_{3\omega}, \tag{2}$$

where B and C are given as

$$B = \frac{256\pi^4}{c^2(n_\omega^2 - n_{3\omega}^2)^2}(\chi^{(3)})^2T^2t^6I_\omega^3, \tag{3}$$

and

$$C = \frac{3\pi}{\lambda_\omega}|n_{3\omega} - n_\omega|. \tag{4}$$

Here C is the phase mismatch determined by the difference in the refractive index between the fundamental and TH, c is the light speed, t and T are the transmittance between air and the nonlinear medium for the fundamental and TH, respectively. Eq. (2) can be analytically integrated leading to

$$I_{3\omega} = \frac{B\{2C^2[\exp(-\alpha_{3\omega}z) - \cos 2Cz] + \alpha_{3\omega}C\sin 2Cz\}}{4C^2 + \alpha_{3\omega}^2}. \tag{5}$$

From this equation, the ratio, r, of the TH intensities of the absorptive and absorption-free samples is given by

$$r = \frac{(4C^2 + \alpha_3\omega^2)\sin^2 Cz}{2C^2[\exp(-\alpha_{3\omega}z) - \cos 2Cz] + \alpha_{3\omega}C\sin 2Cz}. \tag{6}$$

Using r together with Eq. (3), the intensity of TH output from the absorptive material is given by

$$I_{3\omega} = \frac{256\pi^4}{c^2}\cdot\frac{1}{(n_\omega^2 - n_{3\omega}^2)^2}\cdot(x^{(3)})^2\cdot T^2\cdot t^6\cdot I_\omega^3\cdot\frac{1}{r}\cdot\sin^2\psi. \tag{7}$$

Here $\psi = Cz_0$, where z_0 is the thickness of the nonlinear material, is the difference in the phase shift between the fundamental and TH brought about by the transmission through the nonlinear material. In this equation the refractive indices were needed to obtain the corrected TH intensity, using the Kramers–Kronig relations [17].

3.2. Detector sensitivity and reference samples

The measurement of the fundamental and TH were made in the IR and visible ranges, respectively. However no detector and spectrometer are sensitive throughout these ranges. As a consequence, two detectors were used in the present measurement; CCD was used for visible, and PtSi detector was used for near-IR (Fig. 1). The spectral sensitivities of both detectors were calibrated with a calibrated curve of spectral luminosity sensitivity of a standard lamp.

Taking into account the calibration curve, the TH intensity can be given by

$$\begin{aligned} I'_{3\omega}/P_{3\omega} &= \frac{256\pi^4}{c^2}\cdot\frac{1}{(n_\omega^2 - n_{3\omega}^2)^2}\cdot(x^{(3)})^2\cdot T^2\cdot t^6\cdot(I'_\omega/Q_\omega)^3\cdot\frac{1}{r}\cdot\sin^2\psi \\ &= A\cdot\left(\frac{l_c}{\lambda_\omega}\right)^2\cdot f(n_\omega,n_{3\omega})\cdot(I'_\omega/Q_\omega)^3\cdot(x^{(3)})^2\cdot\sin^2\psi, \end{aligned} \tag{8}$$

$$f(n_\omega,n_{3\omega}) = \frac{t^6\cdot T^2}{r}. \tag{9}$$

Here I'_ω and $I'_{3\omega}$ are fundamental and TH intensity outputs of the detector, respectively, l_c is the coherent length. Q_ω and $P_{3\omega}$ are the wavelength-dependent sensitivity of the detector for near-IR and visible, respectively, and A is a constant. Nonlinear susceptibility is given by

$$x^{(3)} = \sqrt{\frac{\lambda_\omega^2\cdot I'_{3\omega}/P_{3\omega}}{A\cdot l_c^2\cdot f(n_\omega,n_{3\omega})\cdot(I'_\omega/Q_\omega)^3\cdot\sin^2\psi}}, \tag{10}$$

where I_ω is the intensity of the fundamental output from the absorptive material. A standard sample was used to determine the nonlinear susceptibility due to the complexity of determining the absolute values of I_ω and $I_{3\omega}$. In that case, the nonlinear susceptibility is expressed as

$$\chi_s^{(3)} = \sqrt{\left(\frac{l_{c,r}}{l_{c,s}}\right)^2\cdot\frac{f_r(n_\omega,n_{3\omega})\cdot\sin^2\psi_r}{f_s(n_\omega,n_{3\omega})\cdot\sin^2\psi_s}\cdot\frac{I'_{3\omega,s}}{I'_{3\omega,r}}}. \tag{11}$$

$l_{c,r}$ and $l_{c,s}$ are the coherent lengths of the reference and the sample, respectively, ψ_X, (X = r, s), is the difference in the phase shift between fundamental and TH, and $I_{3\omega,X}$, (X = r, s), is the intensity of TH, for the reference (r) and the samples (s). Neither $P_{3\omega}$ and Q_ω, nor I_ω appear in this equation. By measuring the TH spectra of the reference material and samples using the apparatus with a common configuration, we obtained the spectrum with a minimum error.

3.3. Reference nonlinear materials

The dependence of nonlinear susceptibility on the wavelength of the input pulse and the non-negligible absorption coefficient in the reference material both lead to an error in the nonlinear susceptibility of the samples. Fundamental and TH, therefore, are required to be non-resonant to the transition in the reference materials. In this case, however, the nonlinearity of the reference material is relatively small and gives only a weak reference signal of the third harmonic. Usually fused silica is used as a reference material, but its third-order nonlinear susceptibility, $\chi_r^{(3)}$, is as small as 1.0×10^{-14} esu. We measured the third harmonic spectra with our femtosecond continuum, but the TH signal was too weak as a reliable reference. This is because of the low peak intensity of the incident continuum, which is spectrally broadened and temporally dispersed due to the group dispersion. This chirp is crucial to obtain the TH (degenerate) generation spectrum without serious contamination of sum frequency generation (non-degenerate), which will be discussed in Section 3.4.

Therefore, a nonlinear material with large nonlinearity and no absorption in the visible and near-IR ranges is desirable for our purpose. We found that high-refractive index glasses FDS9 and FD2 satisfy these requirements. The $|\chi^{(3)}|$ spectra of these glasses measured by a conventional method are shown in Fig. 3. The frequency dependence of $|\chi^{(3)}|$ in both glasses seem to be nearly negligible. To obtain an intense and reliable enough reference signal, we applied FDS9 as a standard because its nonlinearity was higher than the other.

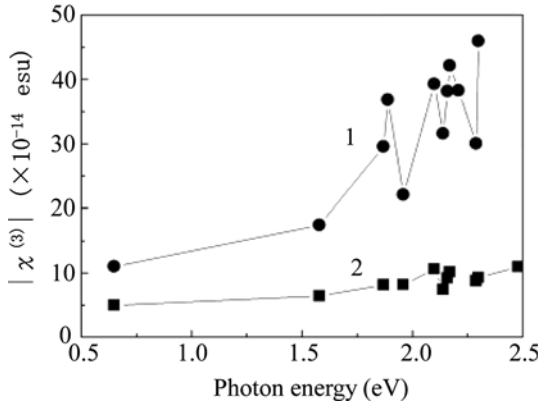

Fig. 3. Nonlinear susceptibility of high-refractive index glasses. (1) FDS9 and (2) FD2. Data for 0.65 eV photon energy was obtained by use of the difference frequency of a YAG laser and a dye laser.

3.4. Contribution of non-degenerate three-wave sum frequency to the TH signal

We used white-light continuum to obtain the $|\chi^{(3)}|$ spectra of the samples, and contribution of the non-degenerate three-wave sum frequency (3-WSF) was carefully investigated. Due to the broad spectrum of the fundamental pulse, the nonlinear polarization at 3ω is given, instead of Eq. (1), by

$$P_{\mathrm{THG}}(r,t) = \int_{-\infty}^{\infty} \mathrm{d}t_1\,\mathrm{d}t_2\,\mathrm{d}t_3 \int_{-\infty}^{\infty} \mathrm{d}\omega_1\,\mathrm{d}\omega_2 \chi^{(3)} \times (-3\omega : \omega_1, \omega_2, 3\omega - \omega_1 - \omega_2) \cdot E_{\omega 1} \times (r, t - t_1) \cdot E_{\omega 2}(r, t - t_2) \cdot E_{3\omega-\omega 1-\omega 2}(r, t - t_3) \quad (12)$$

Hence the output pulse with frequency 3ω can be generated by non-degenerate 3-WSF of three different frequency components, when their sum is equal to 3ω. To exclude the contribution from this process, we used a chirped idler pulse generated by the parametric amplification in the BBO crystal.

In Eq. (12), t_1, t_2, and t_3 are the arrival times of frequency components of the amplified idler pulse at the position r. We measured the chirp property of the amplified pulse by the conventional cross-correlation method. The fundamental idler was mixed with the amplified Ti–sapphire fundamental at 775 nm in the BBO crystal to generate sum frequency through the second-order nonlinear process. From the cross-correlation traces, it was found that time delay between the components at 1700 and 1800 nm is ~220 fs, and the difference in the arrival time between 1800 and 1900 nm is ~250 fs. Since the white-light continuum was generated in CCl_4, which was far off-resonant in the range of the generated continuum, the chirp is expected to be linear. Therefore, the chirp rate can be calculated simply from the delay times measured above. The chirp rate is estimated to be ~0.42 nm/fs in average.

Since the thickness of all the samples used in the present study was less than 15 μm, the spectral component that propagates with a relative delay longer than 50 fs × 1.5 = 75 fs does not interact with each other. Therefore, the spectral components with spectral difference more than 30 nm could not interact each other due to the chirp. The spectrum obtained in the present study, therefore, was considered to be averaged over ±15 nm or equivalently ±13 meV.

Non-degenerate 3-WSF had a considerable contribution in FDS9 because the thickness of this glass plate, 0.975 mm, was substantially large. Dependence of the susceptibility, however, on the wavelength was negligible, so $|\chi^{(3)}|$ was assumed to be constant.

3.5. Effect of TH generation by the air

The TH intensity depended on the coherence length as well as $|\chi^{(3)}|$. Since the coherence length of the air in the range of our concern was as long as 5.0×10^4 μm, ~10^4

times larger than that of the reference material, it might affect the TH signal from the reference and/or the sample [18,19]. Care was taken when fused silica was used as a reference, since the value of $|\chi^{(3)}|$ in fused silica was as small as 10^{-14} esu. We measured a spectrum of the TH signal from air (Fig. 4) and found that the THG intensity of air was 100–140 times lower than that of FDS9, as one could expect from the fact that $|\chi^{(3)}|$ of air and FDS9 was $\sim 10^{-18}$ and 1.3×10^{-13} esu [15], respectively. Therefore, it is concluded that this method is feasible to measure the $|\chi^{(3)}|$ of a sample, which has nonlinearity higher than FDS9, without calibrating the contribution from the air to the TH signal.

4. Spectrum of the third-order susceptibility for THG in poly(4BCMU)

Since the pioneering work of Sauteret et al. [20], PDA has received considerable attention in the field of nonlinear optics. Recently, a low-loss single crystal waveguide with a large intensity-dependent refractive index, and directional couplers in an amorphous spin-coated film have been fabricated [21,22]. Wavelength dependence of nonlinear susceptibility needs to be considered for discussion of the availability of polymer materials to optical devices for communications and other applications. Studies of the mechanisms and origins of nonlinearity in polymers are crucial to develop another polymer with larger nonlinearity. For this purpose, ultrafast phenomena in conjugated polymers have been extensively studied [23–28].

THG measurements with PDA have been performed to study pure electronic coherent third-order nonlinearity [29–31]. A detailed discussion on the wavelength dispersion of THG susceptibility was made by Stegeman et al. [29,30], and the spectral dependence of THG and electroabsorption were measured for PDA [31].

Using the apparatus developed in the present study, we measured $|\chi^{(3)}|$ of a film of PDA–4BCMU, as shown in

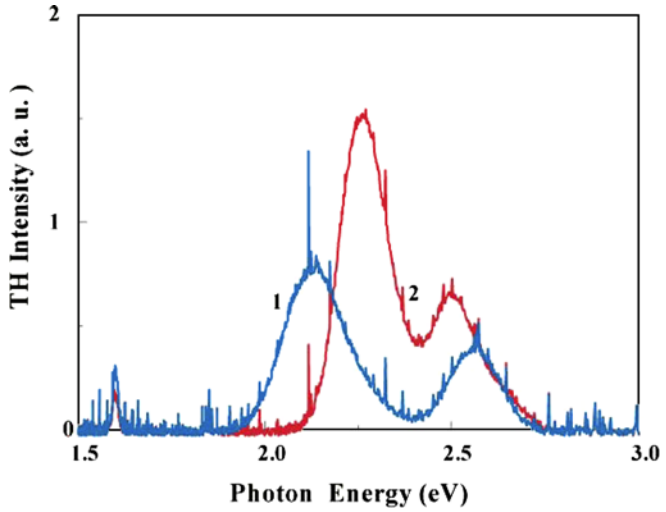

Fig. 4. The spectrum of TH signal from the air with two different wavelength sets (signal, idler). (1) 1.45 and 1.75 μm and (2) 1.49 and 1.65 μm.

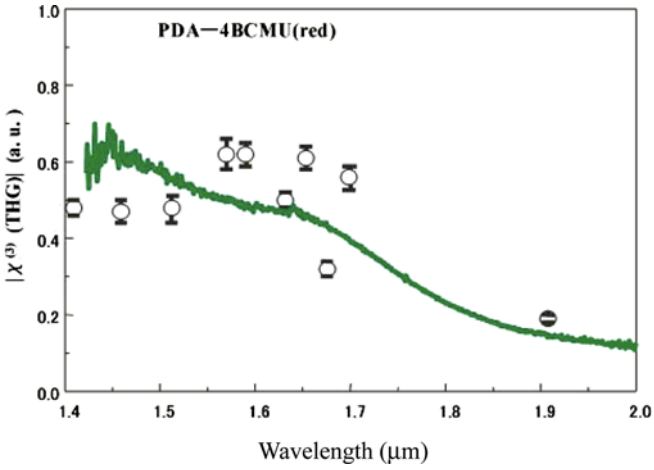

Fig. 5. Experimentally determined $|\chi^{(3)}(3\omega)|$ of poly(4BCMU) in red phase relative to FDS9 together with the data of the polymer determined using fused silica. Reproduced from Ref. [29].

Fig. 5, together with data taken by the point-by-point method in Ref. [29]. The peak value of $|\chi^{(3)}|$ in our measurement was found to be 7.7×10^{-11} esu. Both data have a common feature: $|\chi^{(3)}|$ is larger for shorter wavelength. However, the data obtained by the point-by-point method considerably fluctuate, probably due to systematic errors in the range between 1.5 and 1.7 μm. The scattered data in this range are most probably accidental, since there is no resonance effect that might cause such a fine structure.

Calculations were performed using three-level (3L) and four-level (4L) models [30,31]. In both cases the calculated signal profiles have two peaks or one peak with one shoulder in the calculated range of fundamental, from 0.9 to 1.95 μm. In the 3L model, the ratio of the two peaks at 1.37 and 1.58 μm is 1.29. For the 4L model, the peaks are at 1.34 and 1.60 μm and the intensity ratio is 1.03. It is hard to conclude which of the two models better reproduces the observed result based on the data obtained by the point-by-point method.

The THG $|\chi^{(3)}|$ spectrum obtained in our measurement shows a considerably larger value in the shorter region than that in the longer wavelength region. This supports the result from the 3L model.

5. Conclusion

Wavelength dependence of nonlinear susceptibility of a nonlinear material was measured using a broadband near-IR pulse generated from NOPA, with less systematic error than the conventional method. It was shown that the data obtained by the present method was useful to verify theoretical models.

Acknowledgements

The authors are grateful to Drs. Satoru Shimada and Hiro Matsuda for providing us with the sample of poly(4-BCMU), Prof. Hideki Hashimoto for his valuable discus-

sion. This research is partly supported by a Grant-in-Aid for Specially Promoted Research (#14002003) and partly supported by the program for the Promotion of Leading Researches in Special Coordination Funds for Promoting Science and Technology from the Ministry of Education, Culture, Sports, Science and Technology. This work was also supported by the ICORP program of Japan Science and Technology Agency (JST).

References

[1] D.S. Chemla, J. ZyssNonlinear Optical Properties of Organic Molecules and Crystals, vols. 1 and 2, Academic, New York, 1987.
[2] T. Kobayashi (Ed.), Nonlinear Optics of Organics and Semiconductors, Springer Verlag, Berlin, 1989.
[3] N. Bloembergen, Nonlinear Optics, Benjamin, New York, 1965.
[4] Y.R. Shen, The Principle of Nonlinear Optics, Wiley-Interscience, 1984.
[5] R. Boyd, Nonlinear Optics, second edn., Academic, San Diego, 2003.
[6] S. Takeuchi, T. Kobayashi, J. Appl. Phys. 75 (1994) 2757.
[7] S. Takeuchi, M. Yoshizawa, T. Masuda, T. Kobayashi, IEEE J. Quantum Electron. QE-28 (1992) 2508.
[8] S. Takeuchi, T. Masuda, T. Higashimura, T. Kobayashi, Solid State Commun. 87 (1993) 655.
[9] S. Takeuchi, T. Masuda, T. Kobayashi, Phys. Rev. B, Rapid Commun. 52 (1995) 7166.
[10] A. Shirakawa, T. Kobayashi, Appl. Phys. Lett. 72 (1998) 147.
[11] E. Riedle, M. Beutter, S. Lochbrunner, J. Piel, S. Schenkl, S. Spoerlein, W. Zinth, Appl. Phys. B 71 (2000) 457.
[12] G. Cerullo, M. Nisoli, S. Stagira, S. De Silvestri, Opt. Lett. 23 (1998) 1283.
[13] A. Shirakawa, I. Sakane, T. Kobayashi, Opt. Lett. 23 (1998) 1292.
[14] A. Baltuska, T. Fuji, T. Kobayashi, Opt. Lett. 27 (2002) 306.
[15] A. Mito, K. Hagimoto, C. Takahashi, Nonlinear Opt. Quantum Opt. 13 (1995) 3.
[16] T. Kobayashi, J. Lumin. 53 (1992) 159.
[17] R. Loudon, The Quantum Theory of Light, Clarendon Press, Oxford, 1973.
[18] F. Kajzar, J. Messier, Phys. Rev. A 32 (1985) 2352.
[19] F. Krausz, E. Wintner, Appl. Phys. B 49 (1989) 479.
[20] C. Sauteret, J.P. Hermann, R. Frey, F. Pradere, J. Ducuing, R.H. Baugham, R.R. Chance, Phys. Rev. Lett. 36 (1976) 956.
[21] D.M. Krol, M. Thakur, Appl. Phys. Lett. 56 (1990) 1406.
[22] P.D. Townsend, J. Jackel, G.L. Baker, J.A. Shelburne III, S. Etemad, Appl. Phys. Lett. 55 (1989) 1829.
[23] T. Kobayashi, M. Yoshizawa, U. Stamm, M. Taiji, M. Hasegawa, J. Opt. Soc. Am. B 7 (1990) 1558.
[24] M. Yoshizawa, Y. Hattori, T. Kobayashi, Phys. Rev. B 47 (1993) 3882.
[25] T. Kobayashi, A. Shirakawa, H. Matsuzawa, H. Nakanishi, Chem. Phys. Lett. 321 (2000) 385.
[26] M. Yoshizawa, A. Kubo, S. Saikan, Phys. Rev. B 60 (1999) 15632.
[27] Y. Yuasa, M. Ikuta, T. Kobayashi, Phys. Rev. B 72 (2005) 134302.
[28] Y. Yuasa, M. Ikuta, T. Kobayashi, T. Kimura, H. Matsuda, Phys. Rev. B 72 (2005) 134302.
[29] W.E. Torruellas, K.B. Rochford, R. Aanoni, S. Aramaki, G.I. Stegeman, Opt. Commun. 82 (1991) 94.
[30] M. Cha, W. Torruellas, G. Stegeman, H.X. Wang, A. Takahashi, S. Mukamel, Chem. Phys. Lett. 228 (1994) 73.
[31] K. Takeda, T. Hasegawa, K. Ishikawa, T. Koda, J. Photopolym. Sci. Technol. 6 (1993) 255.